https://doi.org/10.3311/PPee.22595

Periodica Polytechnica Electrical Engineering and Computer Science, 68(1), pp. 1–11, 2024

A High Robust Optimal Nonlinear Control with MPPT Speed for Wind Energy Conversion System (WECS) Based on Doubly Fed Induction Generator (DFIG)

Toufik Mebkhouta[1*], Amar Golea[1], Rabia Boumaraf[1], Toufik Mohamed Benchouia[1], Djaloul Karboua[2]

[1] Laboratory of Electrical Engineering Biskra (LGEB), Department of Electrical Engineering, Faculty of Science and Technology, University of Biskra, P. O. B. 145 RP, Biskra 07000, Algeria
[2] Laboratory of Applied Automation and Industrial Diagnostics (LAADI), Faculty of Sciences and Technology, Ziane Achour University of Djelfa, P. O. B. 3117, 17000 Djelfa, Algeria
* Corresponding author, e-mail: Toufik.mebkhouta@univ-biskra.dz

Received: 15 May 2023, Accepted: 28 July 2023, Published online: 05 October 2023

Abstract

As part of efforts to improve wind energy production using a doubly fed induction generator (DFIG), this paper presents modeling with power maximization through control of speed (MPPT) and control of stator active and reactive power for doubly fed induction generator. The quality of the generated energy and the performance of wind energy conversion systems (WECS) based on DFIG are affected by uncertainties and external disturbances. Therefore, the system requires high-performance control under the nonlinearity influence and the applied external disturbances. This work provides a new contribution and approach that combines nonlinear control (Backstepping) and optimal control (LQR). Backstepping control has been applied to give a good performance using nonlinear strategy and stability condition, but its main drawback is that it is relatively robust for sudden changes in wind speed or any external disturbances as well as it is sensitive against the uncertainties, which may lead to a chattering and an instability as well as overshoot or undershoot. To overcome the problems mentioned above the optimal control (LQR) has been applied to address this drawback in nonlinear control. Furthermore, it, the hybrid approach of Backstepping and LQR control resulting a robust control under the hardest scenarios during the wind system operating as well as provides a good performance in terms of chattering, stability and other performance characteristics which help to produce a high-quality energy. Overall, integrating LQR control with Backstepping can lead to a more powerful, flexible, and efficient control system with improved performance and reduced computational complexity.

Keywords

doubly fed induction generator, active and reactive power, wind energy conversion system, nonlinear control, optimal control, robust control, chattering, stability, high-quality energy

1 Introduction

Recent climate changes have raised serious concerns about their impacts. Due to the large use of fossil energies. As a result, the world is now searching for solutions to reduce the impact climate change, and renewable energy is seen as a good alternative for energy production. Wind energy is one of the most important sources of renewable energy for electricity generation, and its concept revolves around using the movement of air resulting from differences in pressure and temperature distribution in the Earth's atmosphere. Wind energy has many advantages over other energy sources, such as being a clean and renewable source that does not produce harmful or polluting emissions. It is also highly cost-effective in the long run, as the costs of installing and maintaining wind turbines are compensated for over time by the savings in energy costs [1–7].

We can harness this energy to produce electricity using various machines that convert wind energy into electrical energy. The doubly fed induction generator (DFIG) is the most common type of generator used in wind energy conversion systems (WECS). It is known for its ability to provide efficient power generation, especially in low wind speed conditions [8].

However, the DFIG features mentioned above, its torque is designed to a complex and nonlinear model which effect on its performance. For this matter, we need control that ensures good energy production performance.

Cite this article as: Mebkhouta, T., Golea, A., Boumaraf, R., Benchouia, T. M., Karboua, D. "A High Robust Optimal Nonlinear Control with MPPT Speed for Wind Energy Conversion System (WECS) Based on Doubly Fed Induction Generator (DFIG)", Periodica Polytechnica Electrical Engineering and Computer Science, 68(1), pp. 1–11, 2024. https://doi.org/10.3311/PPee.22595

Many control techniques have been applied on the DFIG system successfully, among these controls which depend on the classical regulator "PID" like field-oriented control (FOC) and direct torque control "DTC". Although, they are given a relatively characteristics performance; however, they suffer to the uncertainties like parameters variations and external disturbances like sudden and strong of wind speed change. To overcome these problems, the advanced techniques were used by researchers. The advanced techniques are classified into to the nonlinear like Backstepping and sliding mode, adaptive like model adaptive reference control or MRAC, optimal like linear quadratic regulator "LQR". Many researches were applied the nonlinear control based on Backstepping on the power and current loop of the DFIG where give better characteristic performance compared the classical controls. However, the performance DFIG still suffer to the effects of the uncertainties and external disturbances mentioned above. Other researchers were improved the Backstepping using Fuzzy logic, Adaptive and Sliding mode control where it has been giving more characteristics performance and more robustness but there more combination or hybridization between advanced control techniques in order to exploit the advantages of each technology and avoid its problems. Wherefore, this paper proposed a new design based on a hybrid technique between the optimal and nonlinear control, where the nonlinear depended on the Backstepping (BSC) and the optimal depended on the linear quadratic regulator (LQR). The Backstepping will apply on the power loop of the system which deals with the nonlinearity of the DFIG model easily and ensure its stability by using Lyapunov function candidate. The linear quadratic regulator will apply on the current loop of the DFIG system, where this technique will contribute to improve the DFIG performance and giving optimal characteristics like rise time, steady-state error as well as reducing the chattering and overshoot or undershoots.

Furthermore, of, the new design of the proposed hybrid technique will be robust under the scenarios mentioned above which was effect on the DFIG system [9–15].

This work is divided into several sections. Sections 2 and 3 deal with the modeling of wind turbine and MPPT with speed control, followed by Section 4 dedicated to the modeling of the doubly fed induction generator with several assumptions to facilitate its control. Section 5 is dedicated to the detailed explanation and application of Backstepping control (power loop) while Section 6 explains how to apply optimal LQR (current loop) control generator side. Then, Section 7 shows the results of the applied control, followed by Section 8 that demonstrates the robustness of the proposed control strategy in this work.

The Fig. 1 presents the doubly fed induction generator (DFIG) that has been studied and utilized for WECS in this project, along with numerous details related to the applied control.

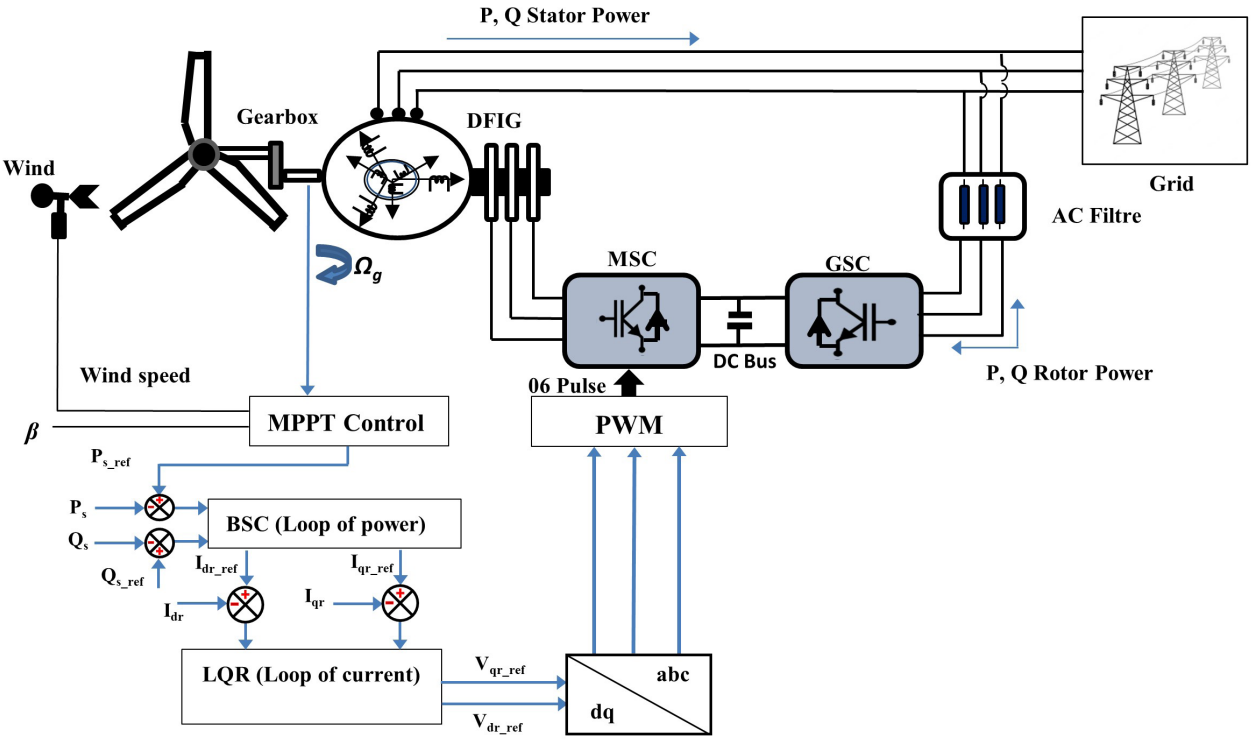

Fig. 1 A wind energy conversion system based on a Doubly Fed Induction Generator

2 Wind turbine model

Wind turbines are machines that use wind energy to generate electricity. These devices are used to convert the kinetic energy from wind into electrical power. They consist of large blades mounted on a rotor, which are connected to a generator that converts the rotational energy into electrical energy. Wind turbines are becoming an increasingly popular source of renewable energy, as they are friendly with the environment and can generate electricity without producing harmful emissions. They can be installed on land (onshore) or on seas and oceans (offshore). Wind turbines are a promising technology that has the potential to significantly reduce our reliance on fossil fuels. The captured power is relative to kinetic energy of air and limited due to the Betz law which is represented by power coefficient C_p described as Eq. (1) and the tip speed ratio λ as Eq. (2), which is the ratio of the linear speed at the blade's tip to the wind speed [16–18].

$$P_{\text{aero}} = \frac{1}{2} C_p(\lambda,\beta)\rho\pi R^2 V^3 \tag{1}$$

$$\lambda = \frac{R\Omega_t}{V} \tag{2}$$

$$C_p(\lambda,\beta) = C_1\left(\frac{C_2}{A} - C_3\beta - C_4\right)e^{-\frac{C_5}{A}} + C_6 \tag{3}$$

3 Maximization of power with speed control

The Fig. 2 is explaining the block diagram of the wind turbine based on MPPT with a speed control where it is adapted from [17].

4 DFIG vector control and modeling: $w_r = w_s - w = gw_s$

The Fig. 3 is describing the DFIG model after performing the Park transformation [17–19]:

$$\begin{cases} V_{ds} = R_s I_{ds} + \dfrac{d\varphi_{ds}}{dt} - w_s\varphi_{qs} \\ V_{qs} = R_s I_{qs} + \dfrac{d\varphi_{qs}}{dt} + w_s\varphi_{ds} \\ V_{dr} = R_r I_{dr} + \dfrac{d\varphi_{dr}}{dt} - w_r\varphi_{qr} \\ V_{qr} = R_r I_{qr} + \dfrac{d\varphi_{qr}}{dt} - w_r\varphi_{dr} \end{cases} \tag{4}$$

$$\begin{cases} \varphi_{ds} = L_s I_{ds} + MI_{dr} \\ \varphi_{qs} = L_s I_{qs} + MI_{qr} \\ \varphi_{dr} = L_r I_{dr} + MI_{ds} \\ \varphi_{qr} = L_r I_{qr} + MI_{qs} \end{cases}. \tag{5}$$

The active and reactive powers at the stator are given by Eqs. (6) and (7) [19, 20]:

$$P_s = V_{ds} I_{ds} + V_{qs} I_{qs} \tag{6}$$

$$Q_s = V_{qs} I_{ds} - V_{ds} I_{qs}\,. \tag{7}$$

Electromagnetic torque is defined by Eq. (8) [20]:

$$T_{em} = \frac{pM}{L_s}\left(I_{dr}\varphi_{qs} - I_{qr}\varphi_{ds}\right). \tag{8}$$

To simplify the system, there steps further before applying the control on our system, it should be some hypothesis for control the output powers of DFIG which are:

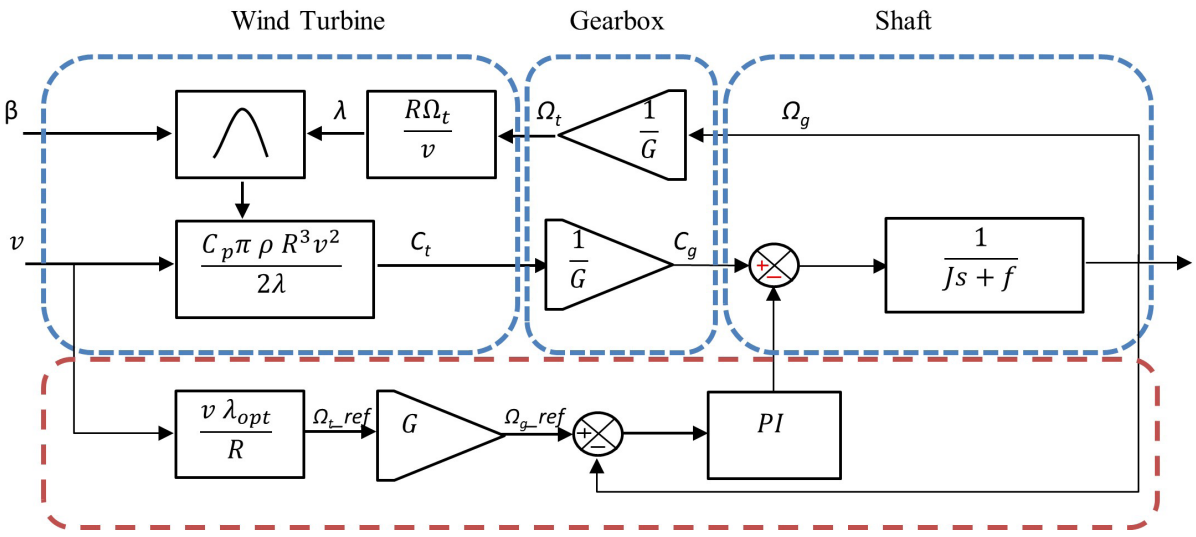

Fig. 2 The block diagram of MPPT with speed control

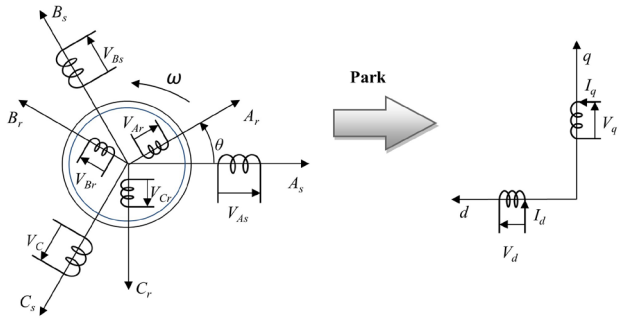

Fig. 3 Park transformation principle applied to DFIG

- By aligning the d-axis in the direction of the stator flux [20, 21] we obtain:

$$\varphi_{ds} = \varphi_s,\ \varphi_{qs} = 0\,. \tag{9}$$

- As a consequence, the stator flux expressions become:

$$\varphi_s = L_s I_{ds} + M I_{dr} \tag{10}$$

$$0 = L_s I_{qs} + M I_{qr}\,. \tag{11}$$

- By neglecting resistances of the stator phases:

$$V_{ds} = 0 \tag{12}$$

$$V_{qs} = V_s = w_s \varphi_s\,. \tag{13}$$

Then rotor currents are used to express stator currents:

$$I_{ds} = \frac{\varphi_s}{L_s} - \frac{1}{L_s} M I_{dr} \tag{14}$$

$$I_{qs} = -\frac{M}{L_s} I_{qr}\,. \tag{15}$$

By using Eqs. (6), (7) and (9) we obtain the active and reactive powers at the stator:

$$P_s = \frac{-V_s M}{L_s} I_{qr} \tag{16}$$

$$Q_s = \frac{-V_s M}{L_s} I_{dr} + \frac{V_s \varphi_s}{L_s}\,. \tag{17}$$

By using Eqs. (8) and (9) we obtain the electromagnetic torque:

$$T_{em} = \frac{pM}{L_s}\left(I_{qr}\varphi_{ds}\right). \tag{18}$$

As a result, the active and reactive powers in the stator are determined by Eq. (19) [20, 21]:

$$\begin{cases} V_{dr} = R_r I_{dr} + a\dot{I}_{dr} - g w_s a I_{qr} \\ V_{qr} = R_r I_{qr} + a\dot{I}_{qr} + g w_s a I_{dr} + g\dfrac{M V_s}{L_s} \end{cases} \tag{19}$$

with $a = L_r - \dfrac{M^2}{L_s}$.

After reaching the simplified equation form of the DFIG, we can draw the block diagram that represent this system, also it should be noted that there is a linkage between the voltages and the active and reactive power by a first order transfer function. The Fig. 4 is describing the block diagram of the simplified DFIG model.

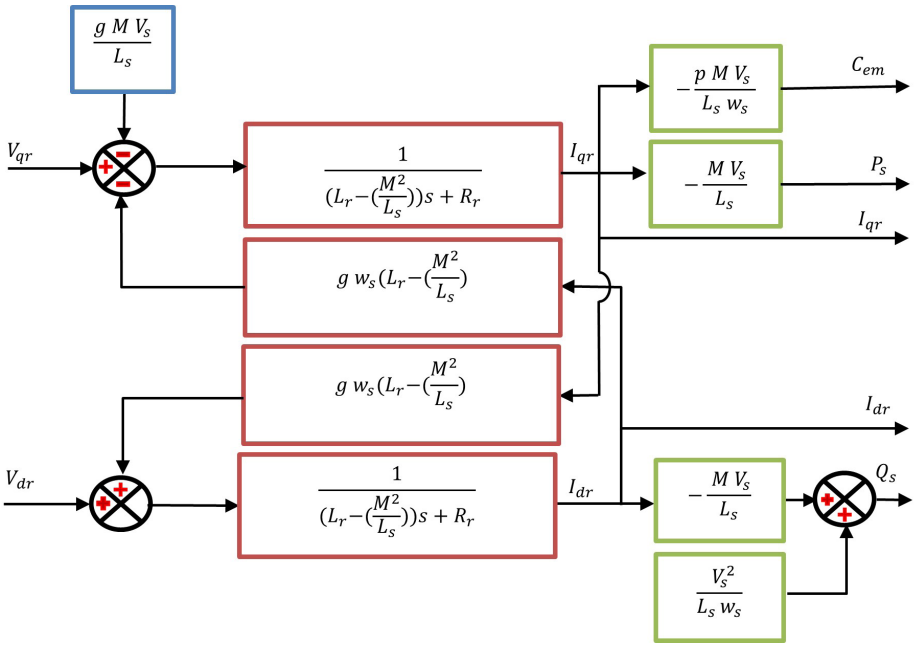

Fig. 4 Block diagram of the simplified DFIG model

5 Design of the BSC based DFIG's loop power

The BSC is one of the most non-linear techniques suggested in the recent years. It depends on study the stabilization to use Lyapunov function for compute the control law. Its object is to reach the zero error convergence, hence, stabilization and equilibration of the system so that the outputs track a reference set point. For this, the active and reactive power of the DFIG is regulated to use the BSC, where the BSC design is based on the FOC with the technique will be applied in the direct and quadratic axes [21, 22].

For current control, direct and quadratic currents are used as manipulated variables to get the law of control. Consequently, the active and reactive tracking error can be specified by Eq. (20) [22]:

$$\begin{cases} \varepsilon_p = P_{s\_ref} - P_s \\ \varepsilon_q = Q_{s\_ref} - Q_s \end{cases}. \tag{20}$$

The BSC used to study the active and reactive power error is based on the Lyapunov candidate as follows:

$$\begin{cases} V_p = \frac{1}{2}\cdot\varepsilon_p^2 \\ V_q = \frac{1}{2}\cdot\varepsilon_q^2 \end{cases}. \tag{21}$$

The deriving of the active and reactive power error represents like following:

$$\begin{cases} \dot{V}_p = \varepsilon_p \cdot \dot{\varepsilon}_p \\ \dot{V}_q = \varepsilon_q \cdot \dot{\varepsilon}_q \end{cases}. \tag{22}$$

To maintain the stability of the system, the requirements must be observed:

$$\begin{cases} V_p > 0, \quad \text{must be} \quad \dot{V}_p < 0 \\ V_q > 0, \quad \text{must be} \quad \dot{V}_q < 0 \end{cases}.$$

To fulfill these conditions, we have:

$$\begin{cases} \dot{\varepsilon}_p = -k_p \cdot \varepsilon_p \\ \dot{\varepsilon}_q = -k_q \cdot \varepsilon_q \end{cases}. \tag{23}$$

And from it the system is stable through the derivative of a negative Lyapunov candidate shown in Eq. (24):

$$\begin{cases} \dot{V}_p = -k_p \cdot \varepsilon_p^2 < 0 \\ \dot{V}_q = -k_q \cdot \varepsilon_q^2 < 0 \end{cases}, \tag{24}$$

where k_p are k_q positive constants.

The reference of the direct and quadratic currents is representing the laws of control, will be given by Eq. (25):

$$\begin{cases} I_{qr_{ref}} = \left(k_p\varepsilon_p + \dot{P}_{s_{ref}}\right)\frac{aL_s}{V_s MR_r} + \left(V_{qr} - gw_s aI_{dr} - g\frac{MV_s}{L_s}\right)\Big/ R_r \\ I_{dr\_ref} = \left(k_q\varepsilon_q + \dot{Q}_{s\_ref}\right)\frac{aL_s}{V_s MR_r} + \frac{V_{dr} + gw_s aI_{qr}}{R_r} \end{cases}. \tag{25}$$

Because the power loop of the DFIG is a nonlinear model, the BSC is applied on it. For that its diagram is designed on the Fig. 5.

6 Design of the LQR based on field oriented of DFIG

The LQR control is applied on the current loop of DFIG model, noting that the model is characterized by MIMO plant and linear state space model, its inputs are direct and quadratic currents and its outputs are direct and quadratic voltages. For this, the DFIG's current loop needs to design using a decoupling method before applying the LQR technique. Where, the DFIG model which represented in the Eq. (19) can be written by Eq. (26):

$$\begin{cases} V_{dr} = V'_{dr} + E_{dr} \\ V_{qr} = V'_{qr} + E_{qr} \end{cases}. \tag{26}$$

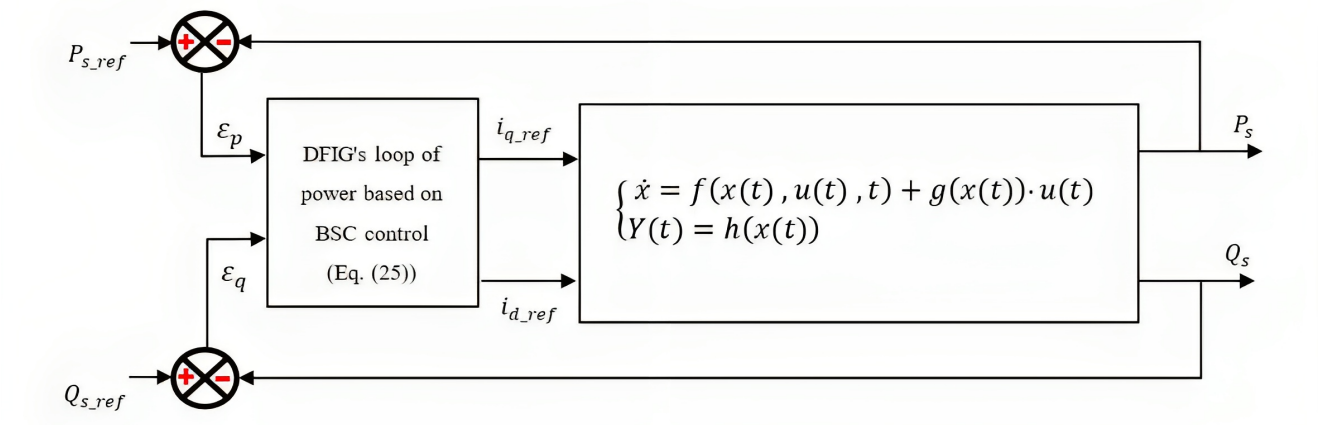

Fig. 5 Design loop of power based on BSC control

Depending on the decoupling method the internal linear model of DFIG is designed in Eq. (27) and the disturbances in the Eq. (28):

$$\begin{cases} V'_{dr} = R_r I_{dr} + a\dot{I}_{dr} \\ V'_{qr} = R_r I_{qr} + a\dot{I}_{qr} \end{cases} \tag{27}$$

$$\begin{cases} E_{dr} = -gw_s aI_{qr} \\ E_{qr} = gw_s aI_{dr} + g\dfrac{MV_s}{L_s} \end{cases}. \tag{28}$$

In the same context, the model mentioned above is designed to use a full state space model following:

$$\begin{cases} \dot{\boldsymbol{x}}(t) = \boldsymbol{A}\cdot\boldsymbol{x}(t) + \boldsymbol{B}\cdot\boldsymbol{u}(t) \\ \boldsymbol{y}(t) = \boldsymbol{C}\cdot\boldsymbol{x}(t) \end{cases}. \tag{29}$$

Based on the Eq. (29) and internal linear model of DFIG of Eq. (27), the DFIG's current loop is written like Eq. (30).

$$\frac{d}{dt}\begin{bmatrix} I_{dr} & I_{qr} \end{bmatrix}^{\mathrm{T}} = \begin{bmatrix} -\dfrac{R_r}{\alpha} & 0 \\ 0 & -\dfrac{R_r}{\alpha} \end{bmatrix}\cdot\begin{bmatrix} I_{dr} & I_{qr} \end{bmatrix}^{\mathrm{T}} + \begin{bmatrix} \dfrac{1}{\alpha} & 0 \\ 0 & \dfrac{1}{\alpha} \end{bmatrix} \cdot\begin{bmatrix} V'_{dr} & V'_{qr} \end{bmatrix}^{\mathrm{T}} \tag{30}$$

The outputs of the current loop model are determined by Eq. (31):

$$\boldsymbol{y}(t) = \begin{bmatrix} 1 & 0 \\ 0 & 1 \end{bmatrix}\cdot\begin{bmatrix} I_{dr} & I_{qr} \end{bmatrix}^{\mathrm{T}}. \tag{31}$$

And the error dynamic is represented in the Eq. (32):

$$\begin{cases} e_{dr} = I_{dr\_ref} - I_{dr} \\ e_{qr} = I_{qr\_ref} - I_{qr} \end{cases}. \tag{32}$$

The controllability study of linear systems is the second stage that comes after modeling the system and before applying the feedback controls. To the current loop become controllable, the basis of this phase must be traced, which is achieved to equality between the rank (r) and the system's order degree (n), because the current loop of the DFIG is a second order system, its controllability matrix is obtained by Eqs. (33) and (34) [23]:

$$P_c = \begin{bmatrix} \boldsymbol{B} & \boldsymbol{AB} \end{bmatrix} \tag{33}$$

$$P_c = \begin{bmatrix} \dfrac{1}{\alpha} & 0 & -\dfrac{R_r}{\alpha^2} & 0 \\ 0 & \dfrac{1}{\alpha} & 0 & -\dfrac{R_r}{\alpha^2} \end{bmatrix}. \tag{34}$$

Since the aforementioned controllability condition is satisfied after calculating a controllability matrix. The state model of the current loop is controllable for all values of the inputs V_{dr} and V_{qr}.

The LQR control has two objectives which makes it dependent on the function cost the under-mentioned and that for built on a quadratic principal to both the characteristics performance regulated by $\boldsymbol{Q}$ matrix and the expenditure of energy of the control signals by $\boldsymbol{R}$ matrix [23, 24]:

$$J = \int_0^{\infty}\left(\left(\boldsymbol{x}^{\mathrm{T}}\cdot\boldsymbol{Q}\cdot\boldsymbol{x}\right) + \left(\boldsymbol{u}^{\mathrm{T}}\cdot\boldsymbol{R}\cdot\boldsymbol{u}\right)\right)dt, \tag{35}$$

where $\boldsymbol{R}$ and $\boldsymbol{Q}$ are positive definite matrices.

Finally, after checking that the current loop is controllable. The Fig. 6 represents the current loop based on the LQR control where a feedback dependent control law is designed like following:

$$\boldsymbol{u}(t) = -\begin{bmatrix} \boldsymbol{K} & \boldsymbol{K}_r \end{bmatrix}\cdot e(t) = \left(-\boldsymbol{R}^{-1}\cdot\boldsymbol{B}\cdot\boldsymbol{P}\right)\cdot e(t). \tag{36}$$

Where $\boldsymbol{P}$ is a positive-definite matrix and is the solution of reduced-matrix Riccati equation represented by Eq. (37) [24]:

$$\boldsymbol{A}^{\mathrm{T}}\cdot\boldsymbol{P} + \boldsymbol{P}\cdot\boldsymbol{A} - \boldsymbol{P}\cdot\boldsymbol{B}\cdot\boldsymbol{R}^{-1}\cdot\boldsymbol{B}^{\mathrm{T}}\cdot\boldsymbol{P} + \boldsymbol{Q} = 0, \tag{37}$$

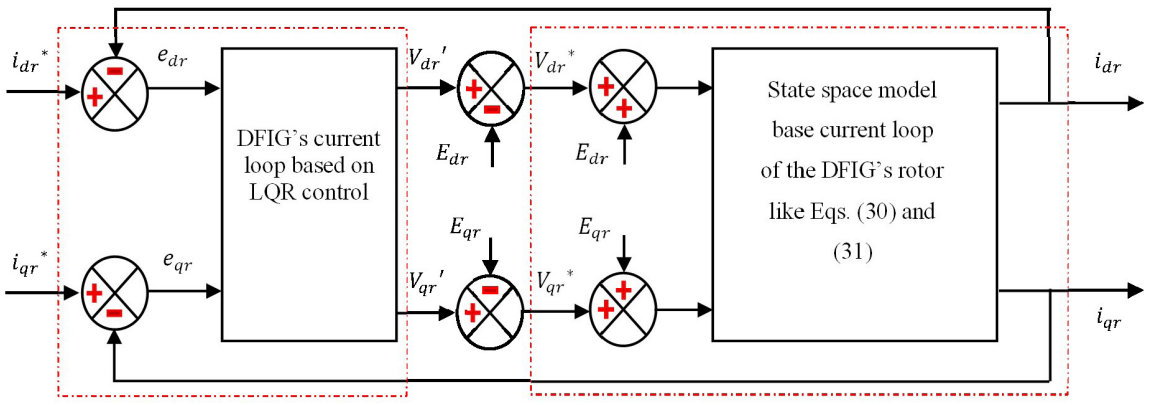

Fig. 6 Current's decoupling model to the DFIG based on a LQR technique

where $\boldsymbol{u}(t)=\left[v'_{dr} \quad v'_{qr}\right]^{\mathrm{T}}$ represents input vector (2 × 1); $\boldsymbol{y}(t)=\left[I_{dr} \quad I_{qr}\right]^{\mathrm{T}}$ represents output vector (2 × 1); $\boldsymbol{x}(t)=\left[I_{dr} \quad I_{qr}\right]^{\mathrm{T}}$ represents state vector (2 × 1); $\boldsymbol{r}(t)=\left[I_{dr\_ref} \quad I_{qr\_ref}\right]^{\mathrm{T}}$ represents reference input vector (2 × 1); $e(t)=\left[e_d \quad e_q\right]^{\mathrm{T}}$ represents error variable state (2 × 1); and $\boldsymbol{A}$ is constant state matrix (2 × 2); $\boldsymbol{B}$ is constant input matrix (2×2); $\boldsymbol{C}$ is constant output matrix (2 × 2); $\boldsymbol{K}$ is optimal feedback matrix (2 × 2); $\boldsymbol{K}_r$ is optimal reference matrix (2 × 2).

7 Results and discussion

Section 7 demonstrates the efficiency of the hybrid technique based on a novel design between the BSC and LQR presented in this paper, where they have been applied on the power and current loop respectively using MATLAB SIMULINK. In the same context, the hardest scenarios of the wind system operating have been validated in Section 7. The first one is considered the external disturbances, where the wind speed change based on large values as well as suddenly like represented in the Fig. 7. Furthermore, the comparison study between the BSC and the proposed control has been represented in the Fig. 8 and Fig. 9 respectively. Despite applying the wind speed mentioned in Fig. 7, the hybrid control (BSC-LQR) in Fig. 9 takes preference through the robustness under the external disturbances as well as the performance through characteristics like zero overshoot and undershoot peaks, rise time and steady-state error. While, the BSC performance in the Fig. 8 suffers from the overshoot and undershoot as follow:

- 6 m/s to 11 m/s: this sudden change in speed is accompanied by an overshoot (+160 var) and an undershoot (−160 var) on Reactive power and an overshoot (*w*) on Active power.
- 11 m/s to 8 m/s: This sudden change in speed also is accompanied by an overshoot (+165 var) and an undershoot (−35 var) on Reactive power and downshoot (*w*) on Active power.
- 8 m/s to 13 m/s: This sudden change in speed also is accompanied by an undershoot (−380 var) on Reactive power and overshoot (*w*) on Active power.

In order to validated the robustness of the proposed control under the uncertainties, the DFIG parameters have been changed during the simulation, which the parameters are R_r and M varied to 50%. Where, the Figs. 10 and 11 are show the results of this scenario.

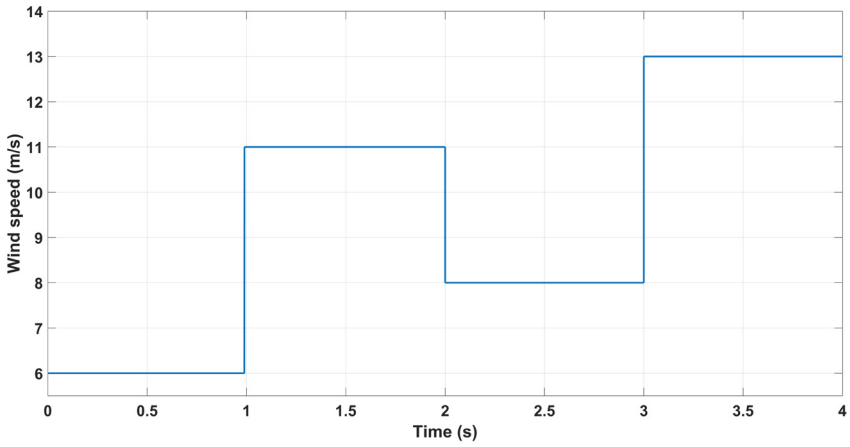

Fig. 7 Wind speed variation

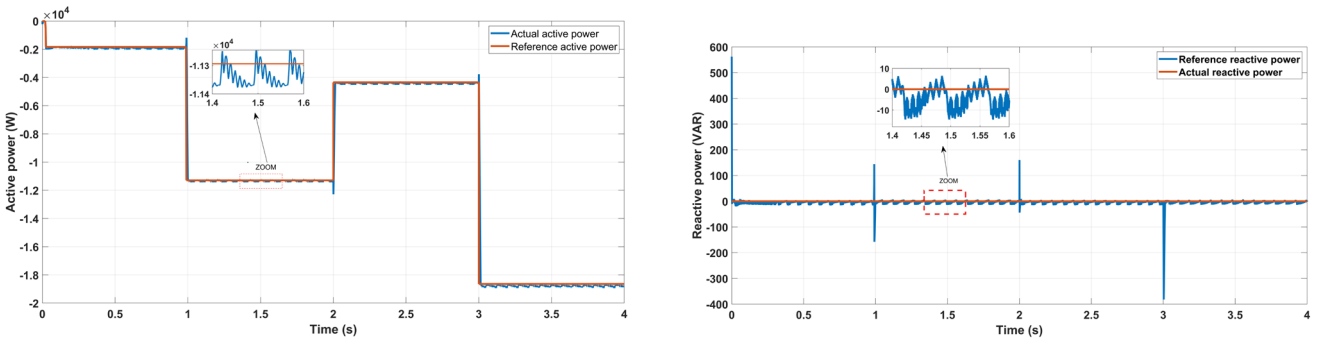

(a) (b)

Fig. 8 Active and reactive power behavior using Backstepping controller

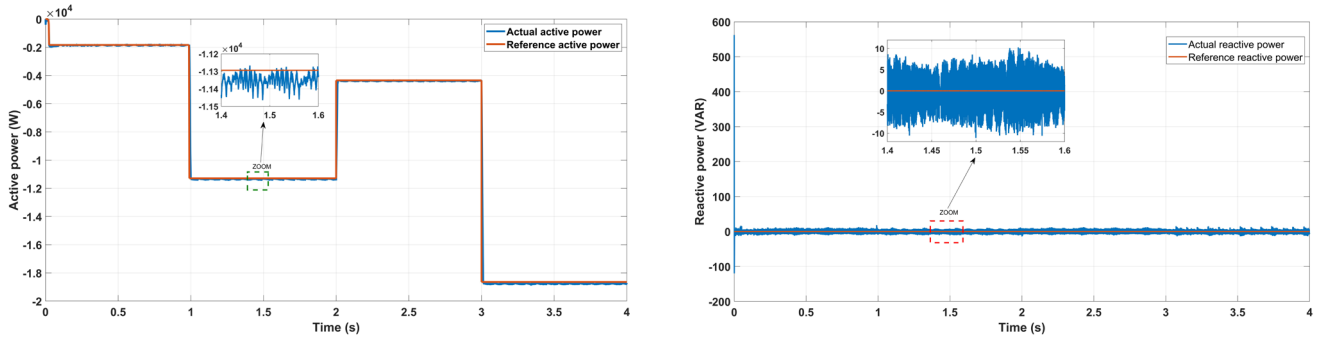

(a) (b)

Fig. 9 Active and reactive power behavior using Backstepping-LQR controller

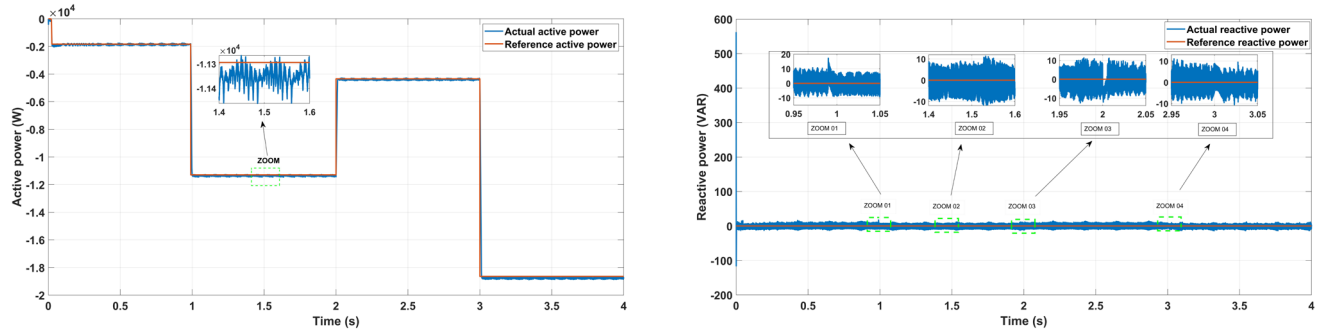

(a) (b)

Fig. 10 Active and reactive power behavior using Backstepping-LQR controller with 50% variation of *Rr*

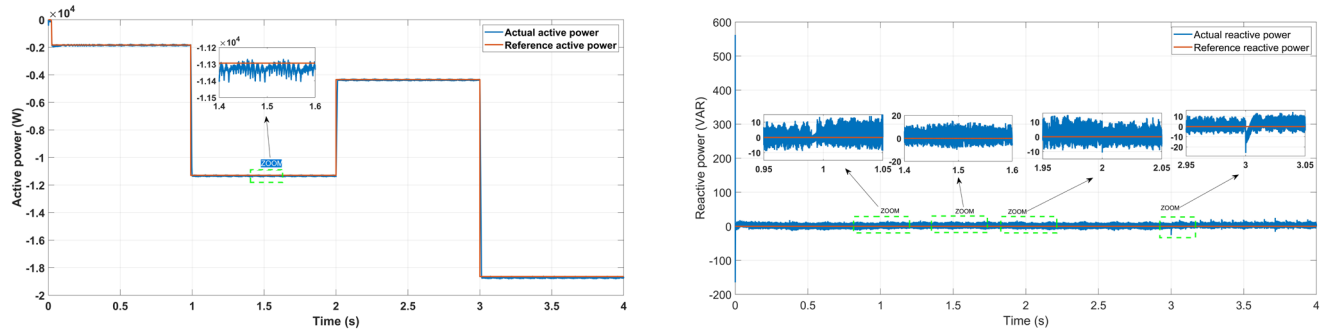

(a) (b)

Fig. 11 Active and reactive power behavior using Backstepping-LQR controller with *M* variation

Through these results, the control provides robustness due to its performance, which hasn't been affected by the uncertainties. Moreover, the proposed control gives good performance characteristics to the active and reactive power like more stability, low chattering, little stead-state error, fast response time.

8 Conclusion

This paper deals with a contribution to the performance improvement of the DFIG control based wind system as well as using MPPT control for the wind turbine, where the hybrid control between the nonlinear Backstepping and optimal linear quadratic regulator has been applied on the DFIG system. Whereas the proposed control has offered good performance characteristics as well as more robust features under the hardest scenarios during the wind system's operation, such as external disturbances and uncertainties like changes in DFIG parameters. Furthermore, the study comparison between the proposed control and the nonlinear technique based on Backstepping control has demonstrated the effectiveness of the proposed control for both characteristic performance and robustness.

References

[1] Ponce, P., Ponce, H., Molina, A. "Doubly fed induction generator (DFIG) wind turbine controlled by artificial organic networks", Soft Computing, 22(9), pp. 2867–2879, 2018. https://doi.org/10.1007/s00500-017-2537-3

[2] Kelkoul, B., Boumediene, A. "Stability analysis and study between classical sliding mode control (SMC) and super twisting algorithm (STA) for doubly fed induction generator (DFIG) under wind turbine", Energy, 214, 118871, 2021. https://doi.org/10.1016/j.energy.2020.118871

[3] Kedjar, B., Al-Haddad, K. "LQR with integral action applied to a wind energy conversion system based on doubly fed induction generator", In: 2011 24th Canadian Conference on Electrical and Computer Engineering (CCECE), Niagara Falls, ON, Canada, 2011, pp. 000717–000722. ISBN 978-1-4244-9788-1 https://doi.org/10.1109/ccece.2011.6030548

[4] Chetouani, E., Errami, Y., Obbadi, A., Sahnoun, S. (2021) "Design of Optimal Backstepping Control for a Wind Power Plant System Using the Adaptive Weighted Particle Swarm Optimization", International Journal of Intelligent Engineering & Systems, 14(6), pp. 125–136, 2021. https://doi.org/10.22266/ijies2021.1231.12

[5] M'zoughi, F., Bouallègue, S., Garrido, A. J., Garrido, I., Ayadi, M. "Water cycle algorithm–based airflow control for oscillating water column–based wave energy converters", Proceedings of the Institution of Mechanical Engineers, Part I: Journal of Systems and Control Engineering, 234(1), pp. 118–133, 2020. https://doi.org/10.1177/0959651818755293

[6] Sudharsan, G. S., Xavier, S. A. E., Raghunathan, V. R. "Fatigue load mitigation in wind turbine using a novel anticipatory predictive control strategy", Proceedings of the Institution of Mechanical Engineers, Part I: Journal of Systems and Control Engineering, 234(1), pp. 60–80, 2020. https://doi.org/10.1177/0959651819850388

[7] Elmouatamid, A., NaitMalek, Y., Bakhouya, M., Ouladsine, R., Elkamoun, N., Zine-Dine, K., Khaidar, M. "An energy management platform for micro-grid systems using Internet of Things and Big-data technologies", Proceedings of the Institution of Mechanical Engineers, Part I: Journal of Systems and Control Engineering, 233(7), pp. 904–917, 2019. https://doi.org/10.1177/0959651819856251

[8] Phan, D. C., Trinh, T. H. "Application of linear quadratic regulator to control directly power for DFIG wind turbine", Journal of Electrical Systems, 15(1), pp. 42–52, 2019. [online] Available at: https://www.proquest.com/openview/13c2f74d1d6c1f425048da7763652f8c/1?pq-origsite=gscholar&cbl=4433095 [Accessed: 17 February 2022]

[9] Salhi, S., Salhi, S. "LQR Robust Control for Active and Reactive Power Tracking of a DFIG based WECS", International Journal of Advanced Computer Science and Applications (IJACSA), 10(1), pp. 565–579, 2019. https://doi.org/10.14569/ijacsa.2019.0100172

[10] Benmeziane, M., Zebirate, S., Chaker, A., Boudjema, Z. "Fuzzy sliding mode control of doubly-fed induction generator driven by wind turbine", International Journal of Power Electronics and Drive System (IJPEDS), 10(3), pp. 1592–1602, 2019. https://doi.org/10.11591/ijpeds.v10.i3.pp1592-1602

[11] Dbaghi, Y., Farhat, S., Mediouni, M., Essakhi, H., Elmoudden, A. "Indirect power control of DFIG based on wind turbine operating in MPPT using backstepping approach", International Journal of Electrical and Computer Engineering (IJECE), 11(3), pp. 1951–1961, 2021. https://doi.org/10.11591/ijece.v11i3.pp1951-1961

[12] Moumani, Y., Laafou, A. J., Madi, A. A. "Modeling and Backstepping Control of DFIG used in Wind Enegry Conversion System", In: 2021 7th International Conference on Optimization and Applications (ICOA), Wolfenbüttel, Germany, 2021, pp. 1–6. ISBN 978-1-6654-3115-6 https://doi.org/10.1109/icoa51614.2021.9442625

[13] Saihi, L., Bakou, Y., Harrouz, A., Colak, I., Kayisli, K., Bayindir, R. "A comparative study between robust control sliding mode and backstepping of a DFIG integrated to wind power system", In: 2019 7th International Conference on Smart Grid (icSmartGrid), Newcastle, NSW, Australia, 2019, pp. 137–143. ISBN 978-1-7281-4859-5 https://doi.org/10.1109/icsmartgrid48354.2019.8990810

[14] Sahri, Y., Tamalouzt, S., Lalouni Belaid, S., Bacha, S., Ullah, N., Ahamdi, A. A. A., Alzaed, A. N. "Advanced fuzzy 12 DTC control of doubly fed induction generator for optimal power extraction in wind turbine system under random wind conditions", Sustainability, 13(21), 11593, 2021. https://doi.org/10.3390/su132111593

[15] Karboua, D., Toual, B., Kouzou, A., Douara, B. O., Mebkhouta, T., Bendenidina, A. N. "High-order Supper-twisting Based Terminal Sliding Mode Control Applied on Three Phases Permanent Synchronous Machine", Periodica Polytechnica Electrical Engineering and Computer Science, 67(1), pp. 40–50, 2023. https://doi.org/10.3311/ppee.21026

[16] Patel, V., Guha, D., Purwar, S. "Chapter 2 - Disturbance observer–aided adaptive sliding mode controller for frequency regulation in hybrid power system", In: Guerrero, J. M., Kandari, R. (eds.) Microgrids: Modeling, Control, and Applications, Academic Press, 2022, pp. 43–66. ISBN 978-0-323-85463-4 https://doi.org/10.1016/b978-0-323-85463-4.00001-0

[17] Chojaa, H., Derouich, A., Chehaidia, S. E., Zamzoum, O., Taoussi, M., Elouatouat, H. "Integral sliding mode control for DFIG based WECS with MPPT based on artificial neural network under a real wind profile", Energy Reports, 7, pp. 4809–4824, 2021. https://doi.org/10.1016/j.egyr.2021.07.066

[18] Radaideh, A., Bodoor, M., Al-Quraan, A. "Active and Reactive Power Control for Wind Turbines Based DFIG Using LQR Controller with Optimal Gain-Scheduling", Journal of Electrical and Computer Engineering, 2021, 1218236, 2021. https://doi.org/10.1155/2021/1218236

[19] Jenkal, H., Bossoufi, B., Boulezhar, A., Lilane, A., Hariss, S. "Vector control of a Doubly Fed Induction Generator wind turbine", Materials Today: Proceedings, 30, pp. 976–980, 2020. https://doi.org/10.1016/j.matpr.2020.04.360

[20] Kelkoul, B., Boumediene, A. "Stability analysis and study between classical sliding mode control (SMC) and super twisting algorithm (STA) for doubly fed induction generator (DFIG) under wind turbine", Energy, 214, 118871. 2021. https://doi.org/10.1016/j.energy.2020.118871

[21] Echiheb, F., Ihedrane, Y., Bossoufi, B., Bouderbala, M., Motahhir, S., Masud, M., ElGhamrasni, M. "Robust sliding-backstepping mode control of a wind system based on the DFIG generator", Scientific Reports, 12(1), 11782, 2022. https://doi.org/10.1038/s41598-022-15960-7

[22] Zeghdi, Z., Barazane, L., Bekakra, Y., Larabi, A. "Improved Backstepping Control of a DFIG based Wind Energy Conversion System using Ant Lion Optimizer Algorithm", Periodica Polytechnica Electrical Engineering and Computer Science, 66(1), pp. 43–59, 2022. https://doi.org/10.3311/ppee.18716

[23] Cheema, M. A. M., Fletcher, J. E., Xiao, D., Rahman, M. F. "A linear quadratic regulator-based optimal direct thrust force control of linear permanent-magnet synchronous motor", IEEE Transactions on Industrial Electronics, 63(5), pp. 2722–2733, 2016. https://doi.org/10.1109/tie.2016.2519331

[24] Sukumaran, S., Arivukkannu, E., Thankappan, S. P., Muthiah, R. "Design of Linear Quadratic Regulator Based Controller for Hybrid Solar-Wind Driven Micro-Grid Inverter", [pdf] Journal of Green Engineering, 10(9), pp. 5380–5400, 2020. Available at: http://www.jgenng.com/wp-content/uploads/2020/11/volume10-issue9-61.pdf [Accessed: 18 February 2022]

Appendix

Fig. A1 and Fig. A2 are presented the result of the stator and rotor currents based on the proposed control and The Table A1 represents DFIG parameters takes from Laboratory of Electrical Engineering Biskra (LGEB), University of Biskra, Algeria.

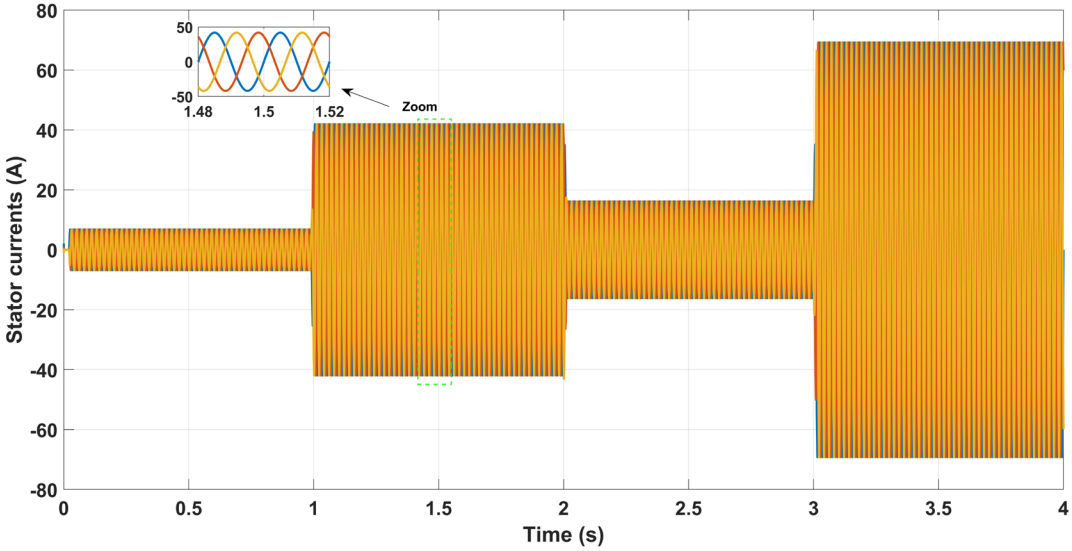

Fig. A1 Stator currents using proposed control Backstepping-LQR

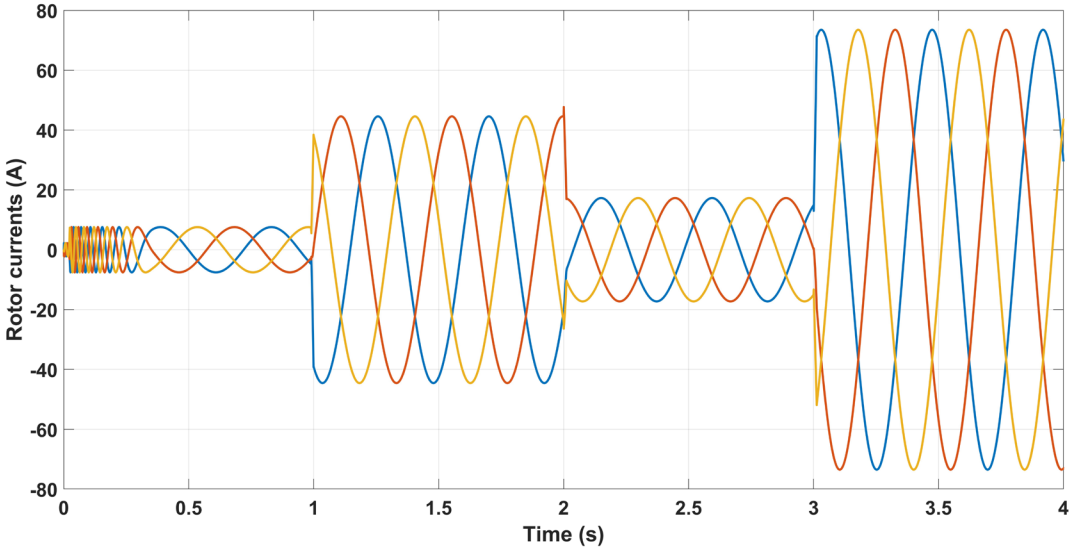

Fig. A2 Rotor currents using proposed control Backstepping-LQR

Table A1 Parameters of the studied system

Parameters	Value
Nominal frequency	50 Hz
Number of pole pair	2
Stator resistance	0.95 Ω
Rotor resistance	1.8 Ω
Stator inductance	0.274 H
Rotor inductance	0.174 H
Mutual inductance	0.258 wb
The inertia	0.1 Kg m^2
Blade radius	5 m
Friction constant	0.0024